RETRIEVING PALEOPOLES USING THE NEW MAPPED LUNAR MAGNETIC ANOMALIES WITHIN BASINS. J. S. Oliveira[1,2] and L. L. Hood[3], [1]ESA/ESTEC, SCI-S, Noordwijk, Netherlands (Joana.Oliveira@esa.int), [2]CITEUC, Geophysical and Astronomical Observatory, University of Coimbra, Portugal, [3]Lunar and Planetary Laboratory, University of Arizona, Tucson, AZ 85721, USA.

Introduction: Orbital spacecraft magnetic field observations show that several isolated magnetic anomalies are found to be heterogeneously distributed over the lunar surface. The most recent global crustal magnetic field maps obtained, have used Lunar Prospector and Kaguya mission data, and have a spatial resolution at the surface of about 6 km [1]. Recently, regional mapping over specific regions related to basins have been performed, as reported in a companion LPSC 2020 abstract [2]. It shows that several details are missing in the previous global model. Further investigations are needed to understand these differences, but we do not exclude an averaging effect that loses small signals when constructing the global models.

Inversions for the magnetization direction to estimate the paleopole positions (defined as the north geomagnetic pole when the anomaly formed) have previously been performed using the global maps [3]. In this study, several isolated anomalies, not specifically related to any geological feature, were used to place constrains on the ancient core field morphology. However, only anomalies that are thermoremanently magnetized are suitable for paleopole inversions, as they hold ancient ambient magnetic field information. Therefore, two questions arise: 1) shall all isolated anomalies be used for retrieving paleopoles to constrain the ancient core field? 2) Are the missing small signals important to constrain the magnetization direction?

In this work, we will study only anomalies that are related to basins/craters. These magnetic anomaly sources are likely to be thermoremanently magnetized. Indeed, it is believed that after the impact, the basin melt sheet cools down slowly recording the ambient magnetic field that is present when the crater formed. We aim to retrieve the paleopole positions using isolated magnetic fields related to basins/craters of the lunar surface. We will compare these results with the previous ones that used global magnetic field models.

Method: We make use of the unidirectional method, developed by [4] to study seamounts on Earth. This approach has been recently applied to other planetary bodies, such as the Moon [3], Mars [5], and Mercury [6]. In detail, a grid of dipoles is placed over the basin inner depression, where the melt sheet is believed to be. All dipoles have the same common direction, following the equation:

$$\boldsymbol{M}\,(\boldsymbol{s}_i) = \hat{\boldsymbol{m}}\, m(\boldsymbol{s}_i), \quad m(\boldsymbol{s}_i) > 0$$

where $\hat{\mathbf{m}}$ is the unit direction of magnetization and $m(\mathbf{s}_i)$ is the dipole moment at vectorial position $\mathbf{s}_i$.

With this, we are assuming that the ambient field was constant in direction when the basin melt sheet cooled below the Curie temperature to become magnetized. A strength of this method is that a unidirectional magnetized volume is mathematically equivalent to a distribution of unidirectional dipoles on the volume's boundary. This property allows to reduce considerably the size of the problem. We apply the non-negative least squares approach that naturally finds which dipoles are nonzero, as well as their intensity. Finally, the best fitting magnetization direction is converted to the north magnetic paleopole.

Results: Figure 1, shows preliminary results using regionally mapped basins, for the Mendel-Rydberg anomaly. It shows the topography (left chart), the observed magnetic field strength at spacecraft altitudes (middle chart), and the magnetic moments of the retained dipoles (right chart) in the inversion. The best fitting magnetization direction obtained yields a paleopole position at (284ºE, 3ºS), with a misfit of 0.5 nT. This corresponds to an inclination and declination of 205º, -60º, respectively.

Previous works [7] have obtained a paleopole at (310ºE; 2ºS), which is 26 degrees apart from the paleopole position we obtain here.

Also of interest is the distribution of dipoles obtained here. The stronger dipoles are found to lie southwest of the basin center, consistent with the inferred impactor trajectory from northeast to southwest at an angle from the vertical of less than 60º, as reported by [2]. We note here that previous inversions using the same method [7] have obtained the stronger dipoles positions slightly shifted toward the southern part of the inner depression, but with no particular longitude preference.

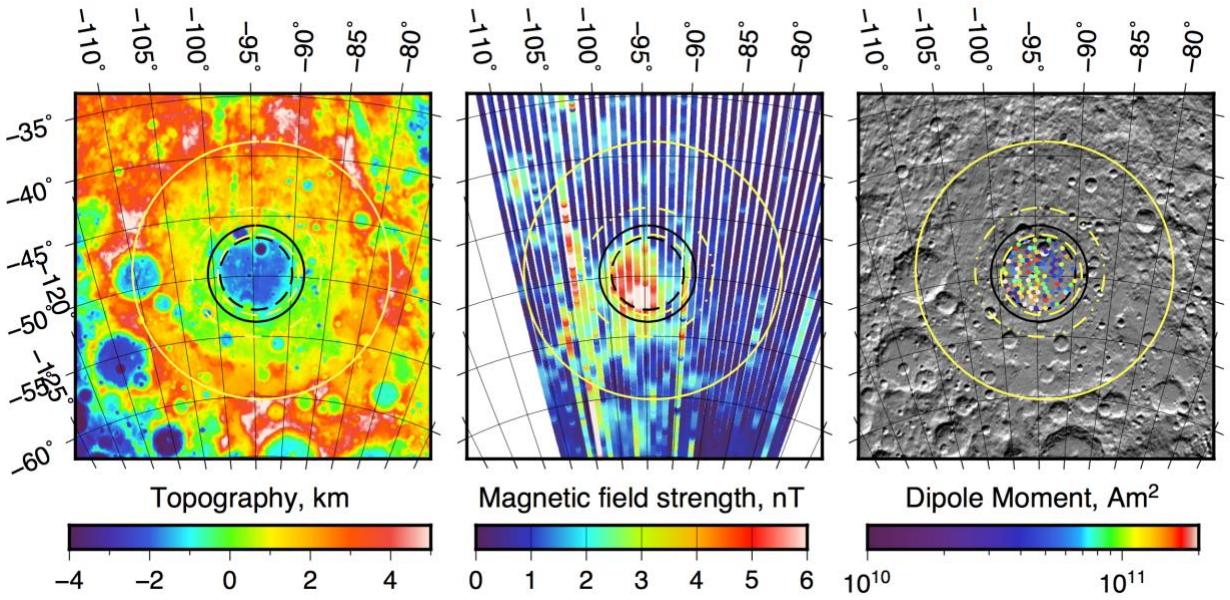

Figure 1: (left) Topography, (middle) observed magnetic field strength at spacecraft altitudes, and (right) the magnetic moments of the retained dipoles in the inversion for the Mendel-Rydberg basin. Yellow circles delimit the basin main rim (solid line), peak ring (dash-dotted line), and inner depression (dashed line) using the diameters of Neumann et al. (2015). Black circles delimit the grid of observations (solid line) and dipoles (dashed line). Images are presented using a Lambert azimuthal equal-area projection.

Conclusions: We show that paleopole position results are highly dependent on the way we construct the magnetic field maps. When applying the Parker's method to the regional mapped magnetic field within Mendel-Rydberg basin, we obtain a different paleopole position when comparing to previous works that have used a global map. We predict larger differences when using other regionally mapped anomalies, such as anomalies within Crisium and Moscoviense basins. It is noteworthy to mention that this study is of extreme importance as these results are the best idea of the ancient core field we have. They will be used to better constrain the lunar ancient core field morphology.

Acknowledgments: This work is supported under a grant (80NSSC18K1602) from the NASA Lunar Data Analysis Program. Maps are from [2] which used Lunar Prospector magnetometer data (available from the Planetary Plasma Interactions node of the NASA Planetary Data System at UCLA) and Kaguya magnetometer data (available from the Japan Aerospace Exploration Agency).

References:

[1] Tsunakawa, H. et al. (2015), JGR Planets, 120, 1160-1185 ;

[2] Hood et al., LPSC 2020-this conference (2020);

[3] Oliveira, J. S. and Wieczorek, M. A. (2017), JGR Planets, 122;

[4] Parker, R. L. (1991) JGR, 96, 16101–16112;

[5] Thomas, P. et al. (2017), JGR Planets, 123, 1140–1155;

[6] Oliveira, J. S. et al., (2019) JGR Planets, 124;

[7] Oliveira J. S. et al. (2017), JGR Planets, 122.